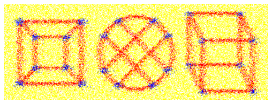
Journal of Graph Algorithms and Applications
http://jgaa.info/ vol. 23, no. 2, pp. 345–369 (2019)
DOI: 10.7155/jgaa.00494

Construction and Local Routing for Angle-Monotone Graphs

Anna Lubiw[1] *Debajyoti Mondal*[2]

[1]Cheriton School of Computer Science, University of Waterloo, Canada
[2]Department of Computer Science, University of Saskatchewan, Canada

Abstract

A geometric graph in the plane is *angle-monotone of width* γ if every pair of vertices is connected by an *angle-monotone path of width* γ, a path such that the angles of any two edges in the path differ by at most γ. Angle-monotone graphs have good spanning properties.

We prove that every point set in the plane admits an angle-monotone graph of width 90°, hence with spanning ratio $\sqrt{2}$, and a subquadratic number of edges. This answers an open question posed by Dehkordi, Frati and Gudmundsson.

We show how to construct, for any point set of size n and any angle α, $0 < \alpha < 45^\circ$, an angle-monotone graph of width $(90^\circ + \alpha)$ with $O(\frac{n}{\alpha})$ edges. Furthermore, we give a local routing algorithm to find angle-monotone paths of width $(90^\circ + \alpha)$ in these graphs. The *routing ratio*, which is the ratio of path length to Euclidean distance, is at most $1/\cos(45^\circ + \frac{\alpha}{2})$, i.e., ranging from $\sqrt{2} \approx 1.414$ to 2.613. For the special case $\alpha = 30^\circ$, we obtain the full-Θ_6-graph and our routing algorithm achieves the known routing ratio 2 while finding angle-monotone paths of width 120°.

Submitted:	Reviewed:	Revised:	Accepted:	Final:
October 2018	February 2019	April 2019	April 2019	April 2019
		Published: April 2019		
	Article type: regular paper		Communicated by: G. Liotta	

This work is partially supported by NSERC. A preliminary version of this paper has appeared at the 44th International Workshop on Graph-Theoretic Concepts in Computer Science (WG 2018) [17].

E-mail addresses: alubiw@uwaterloo.ca (Anna Lubiw) d.mondal@usask.ca (Debajyoti Mondal)

1 Introduction

The problem of constructing a geometric graph on a given set of points in the plane so that the graph is sparse yet has good spanning and/or routing properties has been very well-studied. The basic goal is to guarantee paths that are relatively short, and to be able to find such paths using local routing. Two fundamental concepts in this regard are *spanners* and *greedy graphs*. A geometric graph is a *t-spanner* if there is a path of stretch factor t between any two vertices, i.e., a path whose length is at most t times the Euclidean distance between the endpoints [20]. A geometric graph is *greedy* if there is a path between every two vertices such that each intermediate vertex is closer to the destination than the previous vertex on the path [13]. Greedy graphs permit *greedy routing* where a path from source to destination is found by the local rule of moving from the current vertex to any neighbor that is closer to the destination. However, greedy graphs are not necessarily t-spanners for any constant t.

The most desirable goal would be to construct sparse geometric graphs together with a local routing algorithm to find paths with bounded stretch factor that always get closer to the destination. This is the topic of our paper. There are two aspects to the goal: to construct sparse geometric graphs in which such paths exist, and to find the paths via a local routing algorithm.

Recently, Dehkordi et al. [15] introduced a class of graphs with good path properties: A graph is *angle-monotone* if there is a path between every two vertices that, after some rotation, is x- and y-monotone—equivalently, there is some 90° wedge such that the vector of every edge of the path lies in this wedge. This class was explored (and named) by Bonichon et al. [5]. Any angle-monotone path σ from s to t has the *self-approaching* property (see [1]) that a point moving along σ always gets closer to t. A rich body of research [1, 2, 19, 21, 22] examines self-approaching graphs in various contexts, e.g., finding a self-approaching path in a geometric graph, constructing a self-approaching graph on a given point set, or drawing a graph as a self-approaching graph.

The concept of angle-monotonicity can be generalized to wedges of angles other than 90°—a path is *angle-monotone of width* γ ("generalized angle-monotone") if there is some wedge of angle γ such that the vector of every edge of the path lies in this wedge. Although graphs that are angle monotone of width greater than 90° are not necessarily self-approaching, they have good spanning properties. A graph that is angle-monotone of width $\gamma < 180°$ is a $(1/\cos\frac{\gamma}{2})$-spanner [5], thus a $\sqrt{2}$ spanner for $\gamma = 90°$ (the factor $\sqrt{2}$ is obvious based on the path being x- and y-monotone after some rotation).

Our specific goal in this paper is to construct sparse generalized angle-monotone graphs and design local routing algorithms to find generalized angle-monotone paths in them. There have been a few results on constructing angle-monotone graphs, but no previous results on local routing to find angle-monotone paths—except for some impossibility results.

For more general results on competitive routing, see [12]. Geometric graphs that are useful in this context include Delaunay triangulations [14] and Theta

graphs [10, 6].

Constructing Angle-Monotone Graphs The best result on constructing planar angle-monotone graphs is due to Dehkordi et al. [15] who proved that any set of n points has a planar angle-monotone graph of width 90° using $O(n)$ Steiner points. They proved this by showing that a Gabriel triangulation is angle-monotone of width 90° (see [18] for a simpler proof), and then using the result [3] that any point set can be augmented with $O(n)$ Steiner points to obtain a point set whose Delaunay triangulation is Gabriel. Without Steiner points, it is known that one cannot guarantee planar angle-monotone graphs for all point sets [5]. For the special case of n points in convex position, Dehkordi et al. [15] proved that there exists a (non-planar) angle-monotone graph with $O(n \log n)$ edges. In this paper we show that any point set has an angle-monotone graph with a subquadratic number of edges.

Turning to angle-monotone graphs of larger width, Bonichon et al. [5] showed that the half-Θ_6-graph on a set of n points, which is planar, is an angle-monotone graph of width 120°.

Local Routing on Angle-Monotone Graphs A *k-local routing algorithm* finds a path one vertex at a time using only local information about the current vertex and its k-neighborhood plus the coordinates of the destination. The *routing ratio* of a local routing algorithm is the maximum stretch factor of any path found by the algorithm. The results mentioned in the previous two paragraphs imply that Gabriel graphs are $\sqrt{2}$-spanners, and half-Θ_6-graphs are 2-spanners (as was previously known [6, 14]). Are there local routing algorithms to find paths with good stretch factors, or paths that are angle-monotone in these classes of graphs? The answers are "yes" and "no", respectively. Bonichon et al. [5] gave a 1-local routing algorithm for Gabriel graphs that has routing ratio $(1 + \sqrt{2})$. On the other hand, they proved that no local routing algorithm can find angle-monotone paths in Gabriel graphs.

Bose et al. [10] gave a 1-local routing algorithm for half-Θ_6-graphs that has routing ratio 2.887. They proved that this is the best ratio possible for any local routing algorithm, which implies that no local routing algorithm will find angle-monotone paths of width 120° in half-Θ_6-graphs. We construct a family of graphs together with a local routing algorithm that finds generalized angle-monotone paths.

Contributions Our main results are as follows:

1. Given n points in the plane we construct an angle-monotone graph of width 90° with $O(\frac{n^2 \log\log n}{\log n})$ edges—a subquadratic number of edges. Since angle-monotone graphs are *increasing-chord graphs*, this answers Open Problem 4 from [15].

2. Given n points in the plane and any α, $0 < \alpha < 45°$, we construct an angle-monotone graph of width $90° + \alpha$ with $O(\frac{n}{\alpha})$ edges. We give a 2-local routing algorithm for these graphs that finds angle-monotone paths of

width $90^\circ + \alpha$, thus of stretch factor $1/\cos(\frac{90^\circ+\alpha}{2})$. In particular, for $\alpha = 30^\circ$ our construction yields the full-Θ_6-graph, and our local routing algorithm finds angle-monotone paths of width 120° and stretch factor 2. For this case, our algorithm is 1-local and very similar to the one of Bose et al. [10] that finds paths of stretch factor 2 in half-Θ_6-graphs, but our proof of correctness is simpler.

2 Angle-Monotone Graphs of Width 90°

In this section we show that any set of n points admits an angle-monotone graph of width 90° with $o(n^2)$ edges.

To achieve this, we will use the Erdős-Szekeres theorem [16] to partition the point set into subsets each with a logarithmic number of points in convex position. We will then construct an angle-monotone graph on each pair of subsets. Our construction is inspired by and builds upon a result in [15] that every 'one-sided convex point set' admits an increasing-chord graph with a linear number of edges. In fact, their proof yields an angle-monotone graph of width 90° as we explain in the following section.

2.1 Angle-Monotone Graphs on Convex Point Sets

Dehkordi et al. [15] showed that every convex point set of n points admits an angle-monotone graph with $O(n \log n)$ edges. Actually, they only state that there is an increasing-chord graph. Here we explain why their proof gives the stronger result we need.

A point set P is called *one-sided* with respect to some directed straight line $\vec{d}$, which is not orthogonal to any line through two points of P, if the order of the projections of the points on $\vec{d}$ corresponds to the order the points on the convex-hull of P. Figure 1(a) illustrates a one-sided point set. Given a one-sided point set P with respect to the positive x-axis, Dehkordi et al. [15] showed how to construct a spanning increasing-chord graph G on P with $O(n)$ edges such that any pair of vertices in G are connected by an xy-monotone path. Since xy-monotone paths are angle monotone [1], G is an angle-monotone graph.

Dehkordi et al. [15] used the technique for one-sided point sets recursively to construct increasing-chord graphs on arbitrary convex point sets. They showed that any convex point set P can be partitioned into four one-sided point sets P_1, P_2, P_3, P_4, e.g., see Figure 1(b), such that the following properties hold: (a) The points in each P_i, where $1 \leq i \leq 4$, appear consecutively on the convex hull of P. (b) The partition is balanced, i.e., $\max\{|P_1|+|P_3|, |P_2|+|P_4|\} \leq n/2+1$. (c) The point sets $(P_1 \cup P_2)$, $(P_2 \cup P_3)$, $(P_3 \cup P_4)$, and $(P_4 \cup P_1)$ are one-sided.

Consequently, one can first construct linear-size angle-monotone graphs for one-sided point sets $(P_1 \cup P_2)$, $(P_2 \cup P_3)$, $(P_3 \cup P_4)$, $(P_4 \cup P_1)$, and then recursively construct angle-monotone graphs for the convex point sets $(P_1 \cup P_3)$ and $(P_4 \cup P_1)$. The union of all these graphs contains angle monotone paths for every pair of vertices. Since $\max\{|P_1| + |P_3|, |P_2| + |P_4|\} \leq n/2 + 1$, the size of the final angle-monotone graph is $f(n) \leq 2 \cdot f(\frac{n}{2} + 1) + O(n) \in O(n \log n)$.

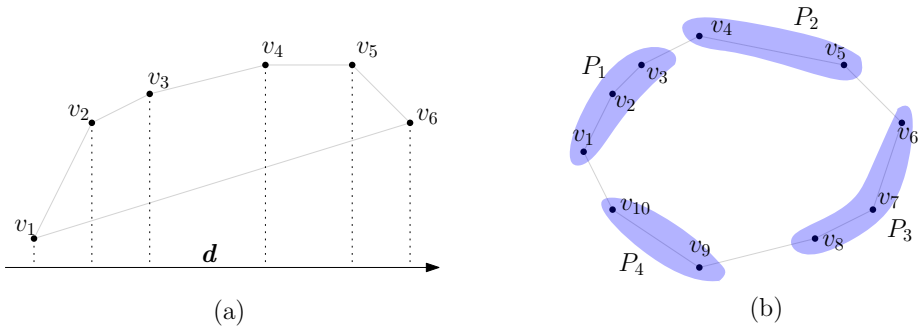

Figure 1: (a) A one-sided convex point set. (b) Illustration for the construction of angle-monotone graphs.

2.2 Angle-Monotone Graphs on Arbitrary Point Sets

We first introduce some preliminary definitions and notation. We will distinguish two types of x-monotone paths: an (x, y)-*monotone path* increases in both x- and y-coordinates, and an $(x, -y)$-*monotone path* increases in x-coordinate and decreases in y-coordinate. For each type of path we further distinguish convex and concave subtypes. Traversed in increasing x order, a convex path turns to the right, and a concave path turns to the left. Thus an (x, y)-*convex path* is an (x, y)-monotone path that turns to the right when traversed in increasing x order, and etc. for the other three types. See Figures 2(a)–(d).

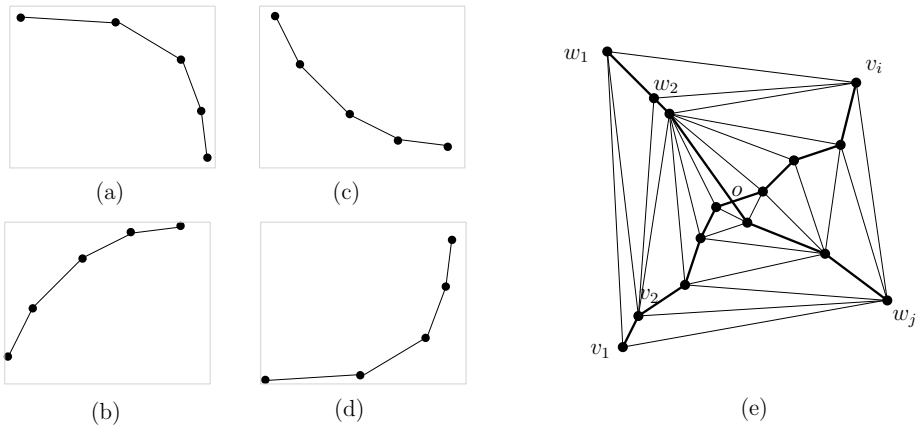

Figure 2: (a) An $(x, -y)$-convex path. (b) An (x, y)-convex path. (c) An $(x, -y)$-concave path. (d) An (x, y)-concave path. (e) Illustration for Lemma 1.

Lemma 1 *Let $P = (v_1, \ldots, v_i)$ be an $(x, -y)$-monotone path, and let $P' = (w_1, \ldots, w_j)$ be an (x, y)-monotone path. Then there exists an angle-monotone graph of width 90° and size $O(i + j)$ that spans P and P'.*

Proof: Assume without loss of generality that P and P' intersect, say at point o. (If necessary, we can add points $(-\infty, \infty)$ and $(\infty, -\infty)$ at the start and end of P respectively, and similarly for P'.) We will solve four subproblems for the points to the left of o, to the right of o, above o and below o, as illustrated in Figure 2(e). Observe that any two points in $P \cup P'$ either lie in the same path, or in one of these half-planes, so it suffices to find an angle-monotone graph of size $O(i + j)$ for each subproblem, and take the union.

Let $v_1, \ldots, v_{i'}$ and $w_1, \ldots, w_{j'}$ be the vertices to the left of the vertical line through o. We now construct an angle-monotone graph spanning these vertices as follows. Add an edge (v_1, w_1) and then move a vertical sweep-line ℓ from $(-\infty, 0)$ to o. Each time we encounter a new vertex q, we add the edges (q, v') and (q, w'), where v' (resp., w') is the rightmost vertex of P (resp., P') lying in the left half-plane of ℓ. We call v' and w' the *predecessor* of q in P and in P', respectively. The resulting graph H has size $O(i + j)$. We now show that H is an angle-monotone graph. For any pair of vertices a, b, if a, b belong to the same path, i.e., P or P', then they are already connected by an angle-monotone path. Otherwise, assume without loss of generality that $a \in P$, $b \in P'$, and b has a larger x-coordinate than a. Let b' be the predecessor of b in P. Follow the path P from a to b' and then take the edge (b', b). This is an $(x, -y)$-monotone path, and thus angle-monotone (equivalently, of width 90°). □

Lemma 2 *Let $P = (v_1, \ldots, v_i)$ be an $(x, -y)$-convex path, and let R be the region (above P) bounded by P and the leftward and downward rays starting at v_1 and v_i, respectively. Then for any set W of j points in R, there exists a graph G of size $O(i + j)$ such that any pair of vertices $v \in P, w \in W$ is connected by an angle-monotone path of width 90°.*

Proof: Let v_0 be any point on the leftward ray starting at v_1. For each q from 1 to i, let ℓ_q be the ray starting at v_q that lies perpendicular to $v_{q-1}v_q$ and enters region R. Since P is convex, the rays ℓ_q subdivide the region R into regions $R_0, R_1, \ldots, R_i$, e.g., see Figure 3(a). For each point v_q, connect v_q to all the points in region $(R_q \cap W)$. Let G' be the resulting graph including the edges of P. We now claim that for any vertex v_t, $1 \leq t \leq q$, and for any $w \in (R_q \cap W)$ the path $v_t, \ldots, v_q, w$ is an angle-monotone path. If the y-coordinate of w is smaller than that of v_q, then this path is $(x, -y)$-monotone and hence angle-monotone, e.g., see Figure 3(b). Otherwise, one can observe that all edges in the path have vectors that lie in the 90° clockwise wedge between ℓ_q and the line extending (v_{q-1}, v_q), e.g., see Figure 3(c). Thus the path $v_t, \ldots, v_q, w$ is an angle-monotone path.

We construct a graph G'' symmetrically by defining, for each q from i to 1, the perpendicular rays $\ell'_1, \ldots, \ell'_i$ and regions $R'_0, \ldots, R'_i$, as illustrated in Figure 3(d). We construct the final graph G by taking the union of all the edges of G' and G''. It is straightforward to observe that G has at most $(i+2j)$ edges.

To complete the proof, we must show that there is an angle-monotone path from any vertex v_t, $1 \leq t \leq i$, to any $w \in W$. Observe that R_t and R'_{t-1} intersect because P is convex. Therefore, the regions $(R_i \cup \cdots \cup R_t)$ and $(R'_{t-1} \cup \cdots \cup R'_0)$

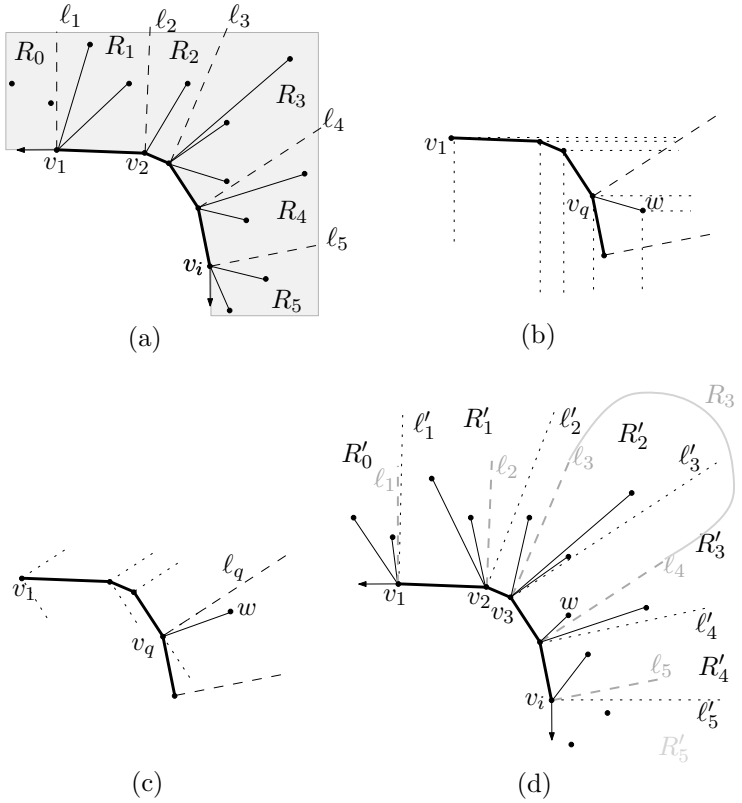

Figure 3: (a)–(d) Illustration for Lemma 2.

together entirely cover the region R. If $w \in (R_i \cup \cdots \cup R_t)$, then there is an angle-monotone path from v_t to w in G', and otherwise $w \in (R'_{t-1} \cup \cdots \cup R'_0)$ and there is an angle-monotone path from v_t to w in G''. □

Lemma 3 *Let $P = (v_1, \ldots, v_i)$ and $P' = (w_1, \ldots, w_j)$ be a pair of $(x, -y)$-convex (or, concave) paths. Then there exists an angle-monotone graph (spanning P and P') with width 90° and size $O(i + j)$.*

Proof: We prove the lemma assuming that P and P' are a pair of convex paths. The case when they are concave is symmetric. We consider two cases depending on whether P and P' intersect or not.

Case 1: First consider the case when P and P' do not intersect, and assume without loss of generality that P' lies in the region above P bounded by P and the leftward and downward rays starting at v_1 and v_i, respectively. Since the vertices on P' are already connected by an angle-monotone path, we can apply Lemma 2 to obtain the required angle-monotone graph.

Case 2: Consider now the case when P and P' intersect. Let $o_1, \ldots, o_t$ be the points of intersections ordered from left to right, e.g., see Figure 4(a). Let

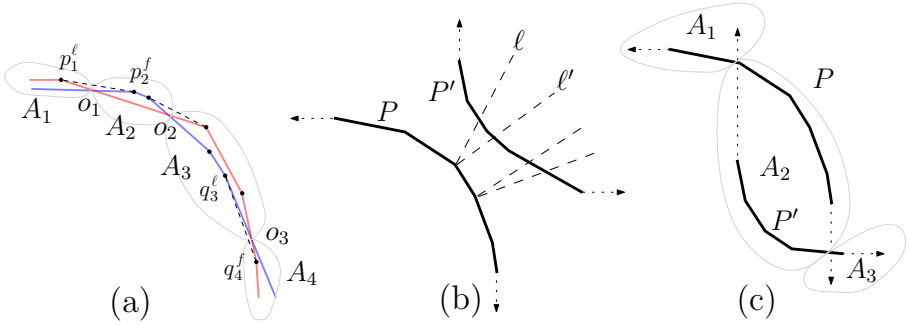

Figure 4: (a)–(c) Illustration for Lemmas 3–4.

A_1 (resp., A_{t+1}) be the set of vertices of $(P \cup P')$ with x-coordinates smaller (resp., larger) than that of o_1 (resp., o_t). For every k, where $2 \leq k \leq t$, let A_k be the set of vertices of $(P \cup P')$ that lie to the left of o_k and to the right of o_{k-1}.

We process the sets $A_1, \ldots, A_{t+1}$ independently using Case 1, and let G_{A_1}, $\ldots, G_{A_{t+1}}$ be the resulting graphs. Finally, we add edges that allow us to transfer from A_k to A_{k+1} above/below each intersection point o_k. Each A_k consists of an upper chain and a lower chain. The lower chains may be empty, but for $1 < k < t+1$ the upper chain of A_k has at least one vertex. For $1 \leq k \leq t$, if these vertices exist, let p_k^f and p_k^ℓ be the first and last vertices of the upper chain of A_k, and let q_k^f and q_k^ℓ be the first and last vertices of the lower chain of A_k. Let T be the set of edges (p_k^ℓ, p_{k+1}^f) and (q_k^ℓ, q_{k+1}^f), for $1 \leq k \leq t$, if these vertices exist. See the dashed edges in Figure 4(a). The final graph G is the union of P, P', $G_{A_1}, \ldots, G_{A_{t+1}}$ and L.

Since P and P' are angle-monotone, we only need to show that every pair of vertices v, w, where $v \in P$ and $w \in P'$ is connected by an angle-monotone path in G. If v and w both belong to the same set A_k, then such a path exists by Case 1. Otherwise, without loss of generality, assume that v belongs to A_k and w belongs to a later set. If v is in the upper chain of A_k then we follow P from v to p_k^ℓ and use the edge (p_k^ℓ, p_{k+1}^f) to transfer to P' and follow it to vertex w. The resulting path is angle-monotone. If v is in the lower chain of A_k and w is not in A_{k+1}, then we can follow P through the upper chain of A_{k+1} and use the edge $(p_{k+1}^\ell, p_{k+2}^f)$ to transfer to P' and follow it to vertex w. Finally, if v is in the lower chain and w is in the lower chain of A_{k+1} then we follow P from v to q_k^ℓ and use the edge (q_k^ℓ, q_{k+1}^f) (which must exist) to transfer to P' and follow it to vertex w. Again, the resulting path is angle-monotone.

The number of edges in G is at most $\sum_{k=1}^{t} O(|A_k|) \in O(i+j)$. □

Lemma 4 *Let $P = (v_1, \ldots, v_i)$ be an $(x, -y)$-convex path, and let $P' = (w_1, \ldots, w_j)$ be an $(x, -y)$-concave path (or, vice versa). Then there exists an angle-monotone graph (spanning P and P') of width $90°$ and size $O(k \log k)$, where $k = \max\{i, j\}$.*

Proof: We extend P by adding leftward and downward rays starting at v_1 and v_i, respectively, e.g., see Figure 4(b). We extend P' symmetrically. We now consider two cases depending on whether P, P' intersect or not.

Case A: If P' and P do not intersect, then P' lies above P. In this scenario we can find an angle-monotone graph of size $O(k)$ by applying Lemma 2.

Case B: If P and P' intersect, then they intersect in at most two points o_1, o_2, with o_1 to the left of o_2, e.g., see Figure 4(c). Let A_1 be the vertices to the left of o_1, A_2 be the vertices between o_1 and o_2, and A_3 be the vertices to the right of o_2. The sets A_1 and A_3 can be handled by Case A. Set A_2 forms a convex polygon bounded by P and P', where the result of Dehkordi et al. [15] gives an angle-monotone graph of size $O(k \log k)$ (see Section 2.1). Finally, for each $t = 1, 2$ we add the edges (p_t^ℓ, p_{t+1}^f) and (q_t^ℓ, q_{t+1}^f) where p_t^ℓ and q_t^ℓ are the last vertices of the upper and lower (resp.) chains of A_t, and p_{t+1}^f and q_{t+1}^f are the first vertices of the upper and lower (resp.) chains of A_{t+1}. The argument that there are angle-monotone paths between every pair of vertices is similar to that in the proof of Lemma 3. □

Theorem 1 *Let S be a point set with n points. Then there exists an angle-monotone graph (spanning S) of width $90°$ and size $O(\frac{n^2 \log\log n}{\log n})$ edges.*

Proof: By the Erdős-Szekeres theorem [16], every point set with n points contains a subset of $O(\log n)$ points in convex position. Urabe [23] observed that by repeatedly extracting such a convex set, one can partition a point set into $O(\frac{n}{\log n})$ convex polygons each of size $O(\log n)$. We partition each of these convex polygons into an (x, y)-convex path, an $(x, -y)$-convex path, an (x, y)-concave path, and an $(-x, -y)$-concave path.

For each pair of these paths, we apply Lemmas 1–4, as appropriate. Finally, we compute the required graph G by taking the union of all the $O(\frac{n^2}{\log^2 n})$ graphs. Since any pair of points in S either lie on the same path, or in one of these $O(\frac{n^2}{\log^2 n})$ graphs, they are connected by an angle-monotone path of width $90°$. Since the length of each path is at most $O(\log n)$, the size of G is $O(\frac{n^2}{\log^2 n}) \cdot O(\log n \log\log n) = O(\frac{n^2 \log\log n}{\log n})$. □

Let S be a point set with t nested convex hulls. Then one can partition these convex hulls into $O(t)$ monotone paths of the form $(\pm x, \pm y)$, each of length $O(n)$. For each pair of these $O(t)$ paths, we can apply Lemmas 1–4, as appropriate, to construct an angle monotone graph of size $O(t^2 n \log n)$ in the same way as we explained in the proof of Theorem 1. Hence we have the following corollary.

Corollary 1 *Let S be a point set with t nested convex hulls. Then there exists an angle-monotone graph (spanning S) of width $90°$ with $O(t^2 n \log n)$ edges.*

2.3 Further Observations

Although the above construction of a subquadratic-size angle-monotone network with width $90°$ is somewhat involved, one can easily construct an angle-

monotone graph with width $(90^\circ + \alpha)$ and $O(\frac{n^{3/2}}{\alpha})$ edges, for any $0 < \alpha \leq 90^\circ$, as we show in this section. In the following Section 3 we give a different construction to obtain a graph with $O(\frac{n}{\alpha})$ edges.

Let S be a set of n points in $\mathbb{R}^2$. To construct an angle-monotone graph, we first mark a set R of $\sqrt{n}$ points from S, and for each pair of points (a, b), where $a \in R$ and $b \in S$, we construct an angle-monotone path of width $90^\circ + \alpha$ between a and b. We then apply this process recursively on $S \setminus R$. We now describe the construction in details. Assume initially all the points of S are unmarked.

Mark a set R of $\sqrt{n}$ points from the unmarked points of S. Let the set of unmarked points be R'. Construct a clique $K_{|R|}$ spanning the points of R. For each point $q \in R'$, create $t = 360^\circ/(2\alpha)$ uniform wedges of angle 2α around q. Figure 5(a) illustrates an example, where the points of R are shown in black. For each wedge W, let $W(R)$ be the points of R that lie inside W. Add an edge between q and the bisector nearest neighbor of q in $W(R)$. Let the resulting graph be H. Note that H has $O(nt) \in O(n/\alpha)$ edges, excluding the edges of the clique determined by R.

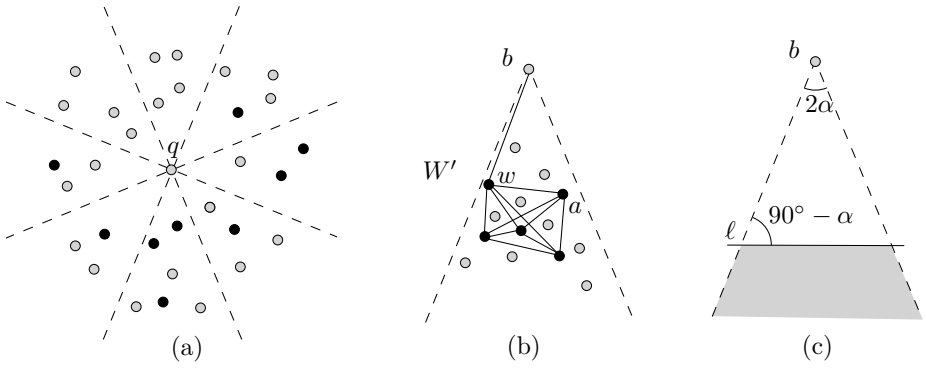

Figure 5: Construction of angle-monotone graphs.

We claim that for each pair of points (a, b), where $a \in R$ and $b \in S$, H contains an angle-monotone path of width $90^\circ + \alpha$ between a and b. If $a \in R$ and $b \in R$, then the claim is straightforward to verify. If $a \in R$ and $b \in R'$, then let W' be the wedge of b that contains a, e.g. see Figure 5(b). Since the points in R form a clique in H, the points of $W'(R)$ form a clique inside W'. Let $w \in W'(R)$ be bisector nearest neighbor of b in W'. If w coincides with a, then (a, b) must be an edge in H. We may thus assume that $w \neq a$. In this scenario, the smallest angle determined by the path a, w, b is at least $(90^\circ - \alpha)$. Therefore, a, w, b is an angle-monotone path of width at most $180^\circ - (90^\circ - \alpha) = (90^\circ + \alpha)$. Figure 5(c) illustrates such a scenario, where the line ℓ passes through w and perpendicular to the bisector of W'. The region where a could be located is shown in gray.

We now apply the above process repeatedly until we mark all the points of

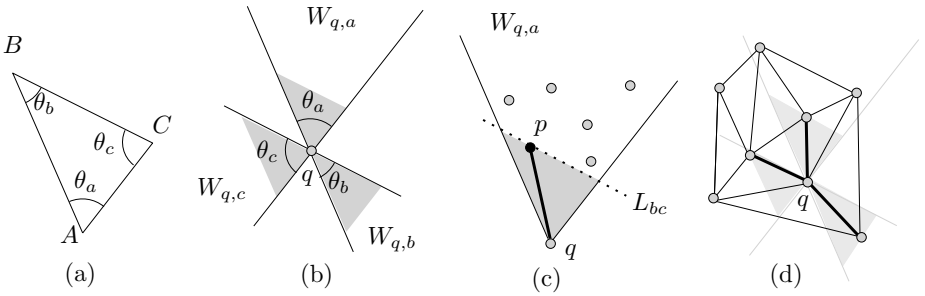

Figure 6: (a) ΔABC. (b) $W_{q,a}, W_{q,b}, W_{q,c}$. (c) The a-nearest neighbor of q, where (q, p) is a θ_a-edge. (d) A 3-sweep graph.

S. Since at each step we process $\sqrt{n}$ new points, the number of steps is $O(\sqrt{n})$. Since at each step we create at most $O(n/\alpha)$ edges, the number of total edges is bounded by $O(\frac{n^{3/2}}{\alpha})$. The resulting angle-monotone graph has diameter 2.

3 Angle-Monotone Graphs of Width $(90^\circ + \alpha)$

In this section we show how to construct, for any point set of size n and any angle α, $0 < \alpha < 45^\circ$, an angle-monotone graph of width $(90^\circ + \alpha)$ with $O(\frac{n}{\alpha})$ edges. We call these *layered 3-sweep graphs*. First, in Section 3.1, we introduce a *3-sweep graph* of a point set in which three lines are used to connect each point to three of its neighbors. The special case where the three lines form 60° wedges yields the half-Θ_6-graph. In Section 3.2, we analyze angle-monotonicity properties of 3-sweep graphs. Then, in Section 3.3, we define a *k-layer 3-sweep graph* as the union of k different 3-sweep graphs. We prove that a layered 3-sweep graph with an appropriate number of layers is an angle-monotone graph of width $(90^\circ + \alpha)$ with $O(\frac{n}{\alpha})$ edges.

3.1 3-Sweep Graphs

Let ΔABC be an acute triangle in $\mathbb{R}^2$ such that A, B, C appear in clockwise order on the boundary of ΔABC, e.g., see Figure 6(a). Let θ_a, θ_b, θ_c be the angles at A, B, C, respectively. For any point q let $W_{q,a}$ (the "a-wedge" of q) be the wedge with apex q such that the two sides of $W_{q,a}$ are parallel to AB and AC, i.e., ΔABC can be translated such that A coincides with q and two sides of ΔABC lie along the sides of $W_{q,a}$. Similarly, we define the wedges $W_{q,b}$ and $W_{q,c}$, e.g., see Figure 6(b). The *a-nearest neighbor* of q in $W_{q,a}$ is defined to be the first point p that we hit (after q) while sweeping $W_{q,a}$ by a line L_{bc} parallel to BC (starting with the line through q). Figure 6(c) illustrates such a sweeping process. In the case of ties, we can pick any of the candidate points arbitrarily as far as the results in this subsection are concerned. However, it is important that the local routing algorithm in Section 4 be able to find the

a-nearest neighbor, so we break ties by choosing the most clockwise point. We call the edge (q, p) a θ_a*-edge*. We define b- and c-nearest neighbors and θ_b- and θ_c-edges analogously.

Given a set of points S, and three angles $\theta_a, \theta_b, \theta_c$ of an acute triangle ΔABC, we define a *3-sweep graph* G *on* S *with angles* $\{\theta_a, \theta_b, \theta_c\}$ to be a geometric graph obtained by connecting every point $q \in S$ to its a-, b- and c-nearest neighbors, e.g., see Figure 6(d). If $\theta_a = \theta_b = \theta_c = 60°$, BC is horizontal, and A is below BC, then G is equivalent to the well known half-Θ_6-graph.

Bonichon et al. [6] proved that half-Θ_6-graphs are equivalent to Triangular Distance (TD) Delaunay triangulations, introduced by Chew [14]. A 3-sweep graph is also the same as the half-Θ_6-graph under a linear transformation. As illustrated in Figure 7, the linear transformation that maps an equilateral triangle T into $T'(= \Delta ABC)$ transforms point set S into S' so that the half-Θ_6 graph on S maps to the 3-sweep graph on S'.

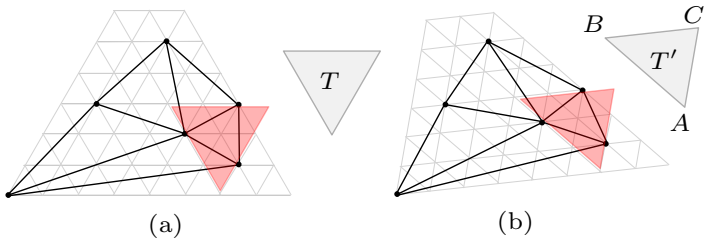

Figure 7: (a) A TD Delaunay triangulation (equivalently, a half-Θ_6-graph) of a point set S, where the neighbors of a vertex are defined based on the sweep distance with respect to the equilateral triangle T. (b) A 3-sweep graph on a point set S' determined by a triangle T', where both S' and T' are transformed using the same linear transformation.

Both half-Θ_6 and 3-sweep graphs are special cases of *convex Delaunay graphs*, which were studied by Bose et al. [7]. They proved that every convex Delaunay graph is a t-spanner, but the value of t obtained from that proof depends on the underlying convex shape, and is very large in our context (e.g., t is bounded by 58 when the convex shape is an equilateral triangle). Every convex Delaunay graph is planar [7], and hence the following lemma is immediate. For interest, here we give a self-contained proof.

Lemma 5 *Every 3-sweep graph is planar.*

Proof: Note that it suffices to prove the following claim.

> Let S be a set of points in $\mathbb{R}^2$, and let q and t be two points in S. Let q' be a nearest neighbor of q in $W_{q,a}, W_{q,b}$, or $W_{q,c}$. Similarly, let t' be a nearest neighbor of t in $W_{t,a}, W_{t,b}$, or $W_{t,c}$. Then the line segments qq' and tt' do not intersect except possibly at their common endpoint, i.e., when $q' = t'$.

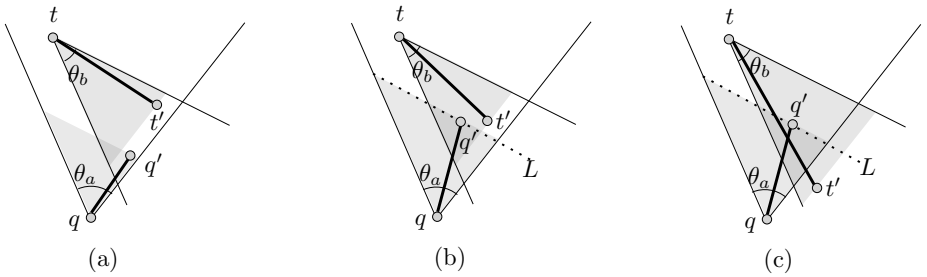

Figure 8: Illustration for the proof of Lemma 5.

The case when $q' \in W_{q,j}$ and $t' \in W_{t,j}$, for some $j \in \{a, b, c\}$ is straightforward. We may thus assume without loss of generality that $q' \in W_{q,a}$ and $t' \in W_{t,b}$, e.g., see Figure 8(a). For convenience, assume that $W_{q,a}$ contains the vertically upward ray starting at q. We now show that the line segments qq' and tt' do not intersect except possibly at their common endpoint, i.e., when $q' = t'$.

Suppose for a contradiction that there exist q, q', t, t' such that the segments qq' and tt' properly intersect. Let r be the point of intersection. Since both $W_{q,a}$ and $W_{t,b}$ contain r and since the left side of $W_{q,a}$ is parallel to the right side of $W_{t,b}$, either $q \in W_{t,b}$ or $t \in W_{q,a}$.

Without loss of generality assume that $t \in W_{q,a}$. Let L be the straight line that passes through q' and makes a clockwise angle of θ_b with the left side of $W_{q,a}$, e.g., see Figure 8(b). Since q' is a nearest neighbor of q, the point t must be on or above L, as otherwise q' would not be the a-nearest neighbor of q. We now consider two cases depending on whether t' is inside or outside of $W_{q,a}$.

If $t' \in W_{q,a}$, then t' must be on or above L . Consequently, tt' may intersect qq' only if t, q' and t' lie on L in this order. Since t' is a nearest neighbor of t, the point q' cannot have smaller distance to t than that of t'. Hence q' must coincide with t', a contradiction.

If $t' \notin W_{q,a}$, then t' must lie to the right of the right side of $W_{q,a}$, e.g., see Figure 8(c). Since t lies on or above L and since qq' intersects tt' inside $W_{q,a}$, q' must lie inside $W_{t,b}$. Consequently, q' must have smaller distance to t than that of t', a contradiction. □

3.2 Angle-Monotonicity of 3-Sweep Graphs

We now analyze angle-monotonicity properties of 3-sweep graphs. We will show that for points q and t in a 3-sweep graph G with t in $W_{q,a}$ there is an angle-monotone path from q to t whose width depends on θ_a and on the position of t relative to the *a-path* of q. The *a-path* of q, denoted $P_{q,a}$, is defined to be the maximal path $(q =)v_0, v_1, \ldots, v_k$ in G such that, for each i from 1 to k, v_i is the a-nearest neighbor of v_{i-1}. We also define the *extended a-path* $\overline{P}_{q,a}$ to be the a-path $P_{q,a}$ together with $W_{v_k,a}$, which is empty of points since the a-path is maximal. We define [extended] b- and c-paths similarly.

Observe that if t is a vertex of $P_{q,a}$ then there is an angle-monotone path of width θ_a from q to t. The following lemma handles the case where $t \in W_{q,a}$, and t does not lie on the a-path from q. The proof of the lemma is very similar to the proof in [5] that the half-Θ_6-graph is angle-monotone of width 120°.

Lemma 6 *Let q and t be two vertices in G such that t lies in $W_{q,a}$. If t lies to the left (resp., right) of $\overline{P}_{q,a}$ then there is an angle-monotone path of width $(\theta_a + \theta_b)$ (resp., $(\theta_a + \theta_c)$) from q to t. Furthermore, the path consists of one subpath of the a-path of q followed by one subpath of the b-path (resp., c-path) of t.*

Proof: Assume that the side BC of ΔABC is parallel to the x-axis and A lies below BC. Such a condition can be met after a suitable rotation of the Cartesian axes. Without loss of generality assume that t lies to the left of $\overline{P}_{q,a}$. We will show that $P_{q,a}$ and $P_{t,b}$ intersect at some vertex x. Our path will then follow $P_{q,a}$ from q to x, and then follow $P_{t,b}$ backwards from x to t. Observe that this path is angle-monotone of width $(\theta_a + \theta_b)$.

Our proof is by contradiction. Assume that $P_{q,a}$ and $P_{t,b}$ do not intersect at a vertex. Let t' be the last vertex of $P_{t,b}$ that lies in $W_{q,a}$ and strictly to the left of $\overline{P}_{q,a}$. Let q' be the last vertex of $P_{q,a}$ that lies below or at the same height (i.e., y-coordinate) as t'.

We will derive a contradiction by considering the possible positions for t' and q'. First suppose that t' is in $W_{q',a}$. See Figure 9(a). Then q' must have an a-nearest neighbor q'', since t' is a candidate to be its a-nearest neighbor. Note that q'' is on $P_{q,a}$. By definition of the a-nearest neighbor, q'' must be at the same height as t', or lower. This contradicts the choice of q' as the last vertex of $P_{q,a}$ that lies below or at the same height as t'.

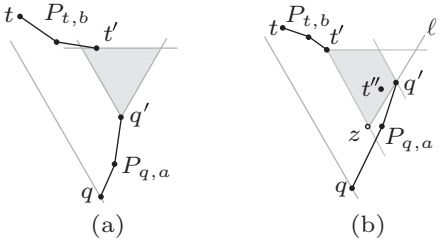

Figure 9: (a) The case of the proof of Lemma 6 when $t' \in W_{q',a}$. (b) The case of the proof of Lemma 6 when $t' \notin W_{q',a}$.

Next suppose that t' is not in $W_{q',a}$. See Figure 9(b). Consequently, q' must be in $W_{t',b}$. Then t' must have a b-nearest neighbor t'', since q' is a candidate to be its b-nearest neighbor. By definition of the b-nearest neighbor, t'' must be to the left of, or on, the line ℓ parallel to AC going through q'. Thus t'' is in $W_{z,a}$ where z is the point where line ℓ intersects the line forming the left side of $W_{t',b}$. If t'' is in $W_{q',a}$ then (as argued above) q' must have an a-nearest neighbor below t', which contradicts the choice of q'.

Thus t'' must lie in the quadrilateral $W_{z,a} - W_{q',a}$ (shaded in Figure 9(b)). Observe that t'' lies in $W_{q,a}$ since both t' and q' do. Finally, we consider whether t'' lies strictly to the left of $\overline{P}_{q,a}$. If t'' lies above q' then it lies strictly to the left of $\overline{P}_{q',a}$ because that portion of the path lies in $W_{q',a}$. So suppose t'' lies below or at the same y-coordinate as q'. Note that t'' cannot lie on the path $q, \ldots, q'$ since we assumed that paths $P_{q,a}$ and $P_{t,b}$ do not intersect at a vertex. If t'' lies strictly to the right of $P_{q,a}$, then path $P_{q,a}$ must contain a point p strictly inside $W_{z,a}$. But then q' is not in $W_{p,a}$, a contradiction since the a-wedge of a point on an a-path must contain all later points of the path. Thus t'' lies strictly to the left of $\overline{P}_{q,a}$. This contradicts the choice of t' as the last vertex of $P_{t,b}$ that is in $W_{q,a}$ and strictly to the left of $\overline{P}_{q,a}$. □

3.3 Layered 3-Sweep Graphs

In this subsection we define an angle-monotone graph of width $(90° + \alpha)$ for any angle α, $0 < \alpha < 45°$, such that $k = \frac{180}{\alpha}$ is an integer, and for any set S of n points. Our graph is defined as a k-layer 3-sweep graph.

Let ΔABC be an acute triangle with A, B, C in clockwise order around the triangle, and with angles $\theta_a = 2\alpha$, $\theta_b = \theta_c = 90° - \alpha$. Orient ΔABC so that the vertically upward ray starting at A bisects θ_a. Let G_1 be the 3-sweep graph of S with respect to the 3 lines through the sides of ΔABC.

We define G_i, $2 \leq i \leq k$ by successive rotations of ΔABC. Let $\Delta_i ABC$ be the triangle obtained by rotating ΔABC clockwise around A with an angle of $\frac{i-1}{k}360°$, and let G_i be the 3-sweep graph of S with respect to $\Delta_i ABC$. The union of $G_1, \ldots, G_k$ is defined to be the *k-layer 3-sweep graph* H_k of S with respect to α.

Theorem 2 *For α, k, S, n as defined above, let H_k be the k-layer 3-sweep graph on S. Then H_k is an angle-monotone graph of width $(90° + \alpha)$ and the number of edges in H_k is $O(\frac{n}{\alpha})$.*

Proof: Let q and v be two points in S. Then v belongs to $W_{q,a}$ in some G_i, where $1 \leq i \leq k$. By Lemma 6, there exists an angle-monotone path of width $2\alpha + (90° - \alpha) = (90° + \alpha)$ between q and v in G_i, and hence also in H_k. By Lemma 5, each G_i is planar. Hence H_k has $O(nk) \in O(\frac{n}{\alpha})$ edges. □

In the remainder of this section we compare k-layer 3-sweep graphs and the more well-known full-Θ_k-graphs, first comparing the number of edges and then the angle-monotonicity. If $2\alpha = 60°$, then $k = 6$. Because of symmetries, $G_i = G_{i+2}$ so we really only have two 3-sweep graphs, and the resulting graph H_6 is the full-Θ_6-graph.

For $k > 6$, H_k may have up to 3 times as many edges as the full-Θ_k-graph. Figure 10(a) illustrates the difference for $k = 10$. However, if k is congruent to 2 mod 4 then the sparser graph determined by the union of $G_2, G_4, \ldots, G_k$ has the same properties as H_k as we now show, using the property that the reverse of an angle-monotone path is also angle-monotone. As already noted in the proof of Theorem 2, for every pair of points $q, v \in S$, v belongs to $W_{q,a}$ in some G_i,

where $1 \leq i \leq k$, and then by Lemma 6, there exists an angle-monotone path of width $2\alpha + (90° - \alpha) = (90° + \alpha)$ between q and v in G_i. If i is even, this path is included in the union of $G_2, G_4, \ldots, G_k$. If i is odd, then, because k is even, q belongs to $W_{v,a}$ in $G_{i+(k/2)}$, where the indices wrap around. Because $k/2$ is odd, the index $i + (k/2)$ is even, and by Lemma 6 there is an angle-monotone path of the required width between q and v in this subgraph.

Every H_k is an angle-monotone graph of width $(90° + \alpha)$, but it is not known whether full-Θ_k-graphs are angle-monotone with bounded width. For every $k = 4m + 4$, where m is a positive integer, one can construct a full-Θ_k-graph of width approximately $(90° + 2\alpha)$. For example, if $k = 8$, then $2\alpha = 45°$, and H_8 is an angle-monotone graph of width 112.5°. A full-Θ_8-graph may have comparatively large width, e.g., Figure 10(b) illustrates a full-Θ_8-graph, where any angle-monotone path between u and v has width approximately 135°.

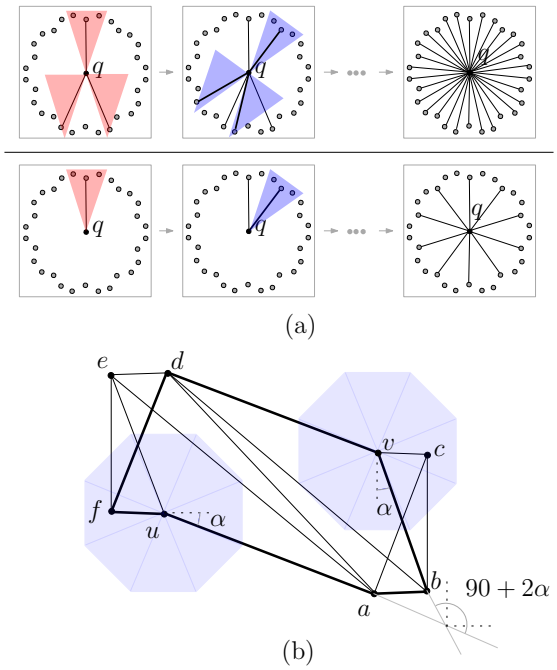

Figure 10: (a) Illustration for the neighbors of q in H_{10} (top), and the full-Θ_{10} graph (bottom). (b) An angle-monotone path between u and v of width approximately $(90° + 2\alpha) = 135°$ (inspired by an illustration in [8]).

4 Local Routing in Layered 3-Sweep Graphs

In this section we give a local routing algorithm for k-layer 3-sweep graphs. Specifically, our routing algorithm is *2-local*, meaning that at each step we assume knowledge of: the coordinates of the current vertex u, the coordinates of

the target vertex, and the *2-neighborhood* of u, which consists of the neighbors of u and their neighbors. In the special case when $k = 6$, i.e., for full-Θ_6-graphs, our routing algorithm is 1-local (see Section 4.1).

Theorem 3 *There is a 2-local routing algorithm that finds angle-monotone paths of width $90° + \alpha$ in any k-layer 3-sweep graph H_k, where $\alpha = 180°/k$. The algorithm has routing ratio $1/\cos(45° + \frac{\alpha}{2})$.*

Before giving the algorithm, we explain why we need 2-locality. Given a start vertex q and a target vertex t, we can find, based on the angle of line qt, which of the k 3-sweep graphs, say G_i, has $t \in W_{q,a}$. Our routing algorithm will only use edges of G_i, so we need a way to tell if an edge of H_k belongs to G_i. Consider an edge from current vertex u to some vertex v. From their coordinates, we can decide whether v is in a *positive* wedge of u in G_i, i.e., one of $W_{u,a}, W_{u,b}$, or $W_{u,c}$ in G_i. If so, then, by checking the other neighbors of u, we can detect if v is the unique a-, b-, or c-neighbor of u in that wedge in G_i. Otherwise, u is in a positive wedge of v in G_i, and, using 2-locality, we can check the neighbors of v to detect if u is the unique a-, b-, or c-neighbor of v in G_i.

For the special case of $\alpha = 30°$, H_k is the full-Θ_6-graph and our algorithm finds angle-monotone paths of width 120° and achieves routing ratio 2. In this case our algorithm, operating on a single 3-sweep graph, can be viewed as a slight variant of the algorithm of Bose et al. [10] for routing positively in a half-Θ_6-graph. Their algorithm achieves spanning ratio 2 but—as stated—includes a tie-breaking rule that prevents it from finding angle monotone paths of width 120°. For the sake of completeness we give an example where the tie-breaking rule in that algorithm causes it to find paths of width arbitrarily close to 180°. See Figure 11(a)–(c). Our contribution is to simplify the statement of the algorithm, generalize to other angles, and give a much simpler proof of correctness using angle-monotonicity.

We briefly mention other approaches to routing. The standard Θ-*routing algorithm* forwards the message from the current vertex v either to the destination (if the destination is adjacent to v), or to the closest vertex in the cone of v that contains the destination. As illustrated in Figure 11(d), the standard Θ-routing algorithm for full-Θ_k-graphs may also yield paths of large width. We refer the reader to [8, Figure 20–22] for more such examples on full-Θ_{4m+4} and full-Θ_{10} graphs. A recent paper by Bose et al. [11] gives yet another local routing algorithm for full-Θ_6-graphs. This algorithm does find angle monotone paths of width 120°, but requires knowledge of the source.

Algorithm $\mathcal{A}$ (Local Routing) Let H_k be a k-layer 3-sweep graph with angles $\theta_a = 2\alpha, \theta_b = \theta_c = 90° - \alpha$, and let q and t be two vertices in H_k.

As discussed above, we can find out which 3-sweep graph, G_i, has t in $W_{q,a}$. We will route in G_i, using 2-locality to distinguish its edges as discussed above. For ease of description, orient the plane with $W_{q,a}$ pointing upward, bisected by the vertical axis, so that edge BC of the reference triangle is horizontal. See

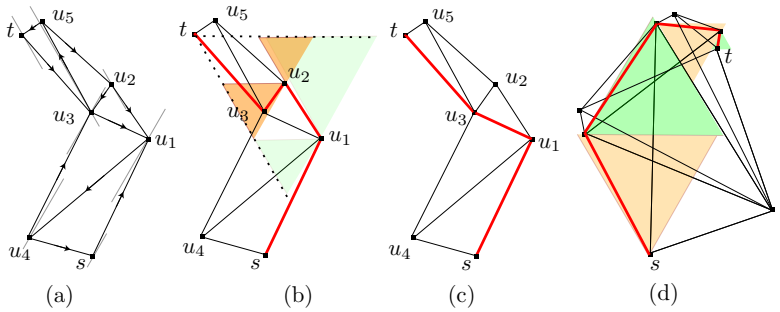

Figure 11: (a) A half-Θ_6-graph G (with arrows indicating the edges into positive cones). (b) The routing algorithm *Algo-half-*Θ_6 of [10] on G takes the path s, u_1, u_2, u_3, t. The edge from u_1 to u_2 is chosen following Case B of *Algo-half-*Θ_6 (the algorithm favors staying close to the largest empty side)[2]. The edge from u_2 to u_3 is chosen following Case C of *Algo-half-*Θ_6. (c) Our algorithm takes the path s, u_1, u_3, t. (d) An example illustrating the standard Θ-routing algorithm on a full-Θ_6-graph.

Figure 12. The general situation is that we have routed (forwarded the message) to some vertex u. Initially $u = q$. The algorithm stops when $u = t$.

- While t is an internal point of $W_{u,a}$, forward the message to u' (i.e., update u to u') where u' is the a-neighbor of u in $W_{u,a}$. See Figure 12(a). Observe that u' is below or on the horizontal line through t.
- After the while loop, u either belongs to $W_{t,b}$ or $W_{t,c}$ (possibly lying on the boundary of the wedge). See Figures 12(b)–(c).
- If u belongs to $W_{t,b}$, call routine $\mathcal{A}_L$, otherwise call routine $\mathcal{A}_R$.

Algorithm $\mathcal{A}_L$ (Left Routing). Invariant: $u \in W_{t,b}$. Until u reaches t do the following:

- Case 1. Forward the message to the first clockwise neighbor v of u in G_i such that $v \in W_{t,b}$ and $u \in W_{v,b}$, if such a vertex v exists. See Figure 12(d).
- Case 2. If no such vertex v exists, then forward the message to vertex u', where u' is the a-neighbor of u in $W_{u,a}$. See Figure 12(e).

Algorithm $\mathcal{A}_R$ (Right Routing). Invariant: $u \in W_{t,c}$. Symmetric to above.

We now prove that $\mathcal{A}$ finds an angle-monotone path of width $(90° + \alpha)$ from the source q to the destination t. Since we execute at most one of $\mathcal{A}_L$ or $\mathcal{A}_R$ and they are symmetric, it suffices to consider the case where $\mathcal{A}_L$ is executed. The significant part of the proof is to show that the algorithm finds a path from q to t. The fact that the path is angle monotone of width $(90° + \alpha)$ follows immediately. In particular, the initial while loop of algorithm $\mathcal{A}$ uses only θ_a-

[2]We note that cases B and D are reversed in the conference version [9] versus the journal version [10].

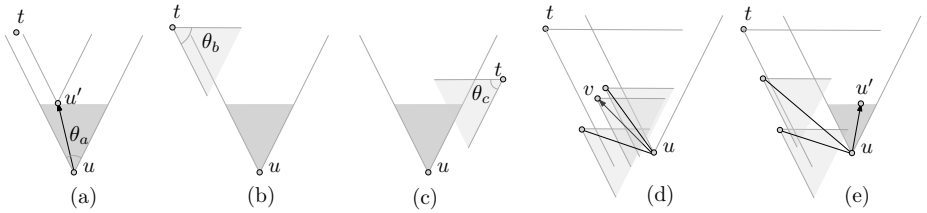

Figure 12: Illustration for algorithm $\mathcal{A}$.

edges, and algorithm $\mathcal{A}_L$ uses only θ_b- and θ_a-edges. Thus the path is angle monotone of width $(90^\circ + \alpha)$. Note that the algorithm does not find a path with θ_a-edges appearing before θ_b-edges, as was guaranteed in Lemma 6.

In order to show that algorithm $\mathcal{A}$ finds a path from q to t we will show: (1) the invariant $u \in W_{t,b}$ holds for algorithm $\mathcal{A}_L$; (2) some measure improves at each routing step of the algorithm.

First consider the invariant $u \in W_{t,b}$. $W_{t,b}$ is bounded by two lines, ℓ and ℓ', where ℓ is the horizontal line through t. To show that $u \in W_{t,b}$, we must show that u is below, or on, ℓ, and to the right of, or on, ℓ'. When we first call $\mathcal{A}_L$, u is to the right of, or on, ℓ', and each step of $\mathcal{A}_L$ preserves this property—see Figures 12(d) and (e). It remains to prove that u is below or on line ℓ. We will prove the stronger invariant that $P_{t,b}$ goes through or above u, i.e. that $P_{t,b}$ intersects the ray going vertically upward from u.

We begin by showing that this is true when we first call $\mathcal{A}_L$. If we call $\mathcal{A}_L$ because q is on ℓ', then $P_{t,b}$ must pass through or above q. The only other way to call $\mathcal{A}_L$ is because we just completed a step of the while loop of $\mathcal{A}$ where t was internal to $W_{u,a}$ but not internal to $W_{u',a}$, e.g., see Figure 12(a). By Lemma 5, $P_{t,b}$ cannot cross the edge (u, u'). Hence it must pass above or through u'.

Now consider a step of $\mathcal{A}_L$ after the first one. We route from u to vertex w which is either vertex v in Case 1 (Figure 12(d)) or vertex u' in Case 2 (Figure 12(e)). Suppose (for a contradiction) that the path $P_{t,b}$ does not go through or above w. By induction we know that $P_{t,b}$ goes through or above u. By Lemma 5, $P_{t,b}$ cannot cross the edge (u, w). (This is where we use the assumption that (u, w) is an edge of G_i.) Thus $P_{t,b}$ must go through u and the other points of edge (u, w) must lie above the path. Let x be the vertex before u on $P_{t,b}$. Then $x \in W_{t,b}$ and $u \in W_{x,b}$. We now claim that the algorithm should have chosen x rather than w. First note that x is a candidate for vertex v in Case 1 of $\mathcal{A}_L$. Thus the algorithm would not have moved to Case 2. Next note that x comes before v in clockwise order around u, so the algorithm would have chosen x rather than v.

It remains to show that something improves at every step of the algorithm. Let d_a be the distance from u to the horizontal line through t. Let d_b be the distance from t to the line determined by the right boundary of $W_{u,a}$. In every iteration of the while loop of $\mathcal{A}$, d_a decreases and d_b does not increase. In Case 2 of $\mathcal{A}_\mathcal{L}$, d_a decreases and d_b does not increase. Finally, in Case 1 of $\mathcal{A}_\mathcal{L}$, d_b

decreases and d_a does not increase. Thus $d_a + d_b$ strictly decreases at every step of the algorithm, and the algorithm must terminate.

4.1 1-Local Routing on Full-Θ_6-Graphs

We observed in Section 3.3 that because of symmetries when $k = 6$ we really only have two 3-sweep graphs, which are in fact two half-Θ_6-graphs which together form a full-Θ_6-graph. For this case, we will show that our routing algorithm is 1-local by showing how to make the message forwarding decisions based on the 1-neighborhood of the current vertex u. Note that the tie-breaking rule that we used to construct the graph for local routing, i.e., by choosing the most clockwise point, remains the same.

Suppose without loss of generality that we are routing in G_1 and are routing from u to t, with $W_{u,a}$ oriented upwards as in the description of Algorithm $\mathcal{A}$. Recall that while t is an internal point of $W_{u,a}$, Algorithm $\mathcal{A}$ forwards the message to u', where u' is the a-neighbor of u in $W_{u,a}$. Since u contains the information about its 1-neighborhood, it is straightforward to make the message forwarding decision.

At this point, we call routine $\mathcal{A}_L$ or $\mathcal{A}_R$ depending on whether u belongs to $W_{t,b}$ or $W_{t,c}$, respectively. By symmetry, it suffices to consider only the left routing $\mathcal{A}_L$.

Case 1 of $\mathcal{A}_L$ forwards the message to the first clockwise neighbor v of u in G_1 such that $v \in W_{t,b}$ and $u \in W_{v,b}$, if such a vertex v exists. See Figure 12(d). We now show how to decide the existence of such a vertex v based on the 1-neighborhood of u.

For any neighbor q of u in G, we can easily test if $q \in W_{t,b}$ and $u \in W_{q,b}$. The issue is whether edge (u, q) lies in G_1 or G_2. Since q lies in a negative cone for G_1, edge (u, q) is in G_1 if and only if u is a b-neighbor of q.

Let R_a (resp., R_b) be the closed region determined by the intersection of $W_{q,b}$ and $W_{u,a}$ (resp., $W_{q,b}$ and $W_{u,c}$). Let R be the closed region inside $W_{q,b}$ bounded by the regions R_a and R_b, as shown in gray in Figure 13(a).

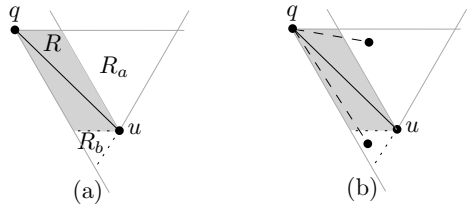

Figure 13: Illustration for the routing in a full-Θ_6-graph.

Since the edge (q, u) corresponds to a nearest neighbor in some cone around either q or u, the region R cannot contain any vertex except for u and q. See Figure 13(b). (This is where we crucially use the fact that G is a full-Θ_6-graph.) Thus u is the b-neighbor of q if and only if both R_a and R_b are empty of any

vertex except for u and q. We can test this (even in the general case) by checking the a- and b-neighbors of u in $W_{u,a}$ and $W_{u,b}$, respectively.

Case 2 of $\mathcal{A}_L$ forwards the message to vertex u', where u' is the nearest neighbor of u in $W_{u,a}$. This case is straightforward since u contains the information about its 1-neighborhood.

The following theorem summarizes the result of this section.

Theorem 4 *There is a 1-local routing algorithm that finds angle-monotone paths of width* $120°$ *in any full-*Θ_6*-graph.*

5 Angle-Monotone Graphs with Steiner Points

The angle-monotone graphs constructed in Sections 2–3 can have a width of $90°$ or larger. Spanning graphs of smaller width can be constructed if we allow Steiner points. For example, any spanning planar triangulation with no angle larger than β is an angle-monotone graph of width β [18]. Since the angles of a triangle sum to $180°$, the best possible value for β is $60°$. We refer the interested reader to [4, 3] for related works on generating meshes with good angle properties. In this section we construct angle-monotone graphs of width γ, for any point set S and any given $\gamma \in (0, 90°]$ where $(360°/\gamma)$ is an integer. However, the size of the graph depends on some distance parameters of the point set.

Here we use a pair of non-obtuse triangles ΔABC and $\Delta A'B'C'$ to construct the angle-monotone graphs, where $\angle BAC$ coincides with $\angle B'A'C'$. Let $\theta_a = \theta_{a'} = \theta_{b'} = \theta_c = \gamma/2$, as illustrated in Figure 14(a). Consider the graph G_{pair} obtained by taking the union of the 3-sweep graphs on S with respect to angles $\{\theta_a, \theta_b, \theta_c\}$ and $\{\theta_{a'}, \theta_{b'}, \theta_{c'}\}$. The following lemma is immediate from Lemma 6.

Lemma 7 *Let* q *and* t *be two vertices in* G_{pair} *such that* t *lies inside* $W_{q,a}$*. If* t *lies to the right of* $\overline{P}_{q,a}$ *(resp., left of* $\overline{P}_{q,a'}$*), then there is an angle-monotone path of width* $(\theta_a + \theta_c) = \gamma$ *(resp.,* $(\theta_{a'} + \theta_{b'}) = \gamma$*) between* q *and* t*.*

Figure 14(b) shows the potential location of t in gray. By Lemma 7, if P_{q,θ_a} coincides with $P_{q,a'}$, then for every point $t \in W_{q,a}$, we can find an angle-monotone path of width γ in G_{pair}. In the following we show how to insert some additional points (i.e., Steiner points) in S such that we can always find such an angle-monotone path. We refer the reader to Figure 14(c). Let $A_0 = A$, and assume for the simplicity of description that the segment BC passes through the a-nearest neighbor q' of q in $W_{q,a}$. We construct a sequence of successive triangles $\Delta A_{i-1}B_iA_i$ (similar to $\Delta A'B'C'$), where for $1 \le i \le k$, the segment $A_{i-1}A_i$ lies on the right side of $W_{q,a}$ and B_i lies on the segment BC, and then place Steiner point s_i at A_i.

We choose k to be the smallest integer such that q' does not belong to $W_{s_k,a}$ (e.g., $k = 3$ in Figure 14(c)), or the a-nearest neighbor of s_k in $W_{s_k,a'}$ coincides with q' (e.g., $k = 1$ in Figure 14(d)). We add the edges (s_{i-1}, s_i), the edge between q' and its corresponding Steiner point s_k, and the edges (z, s_i),

where $z \in S$ and the Steiner point s_i is a b-nearest neighbor of z in $W_{z,b'}$. Let the resulting graph be H, which we will refer to as a *Steiner graph*. Since $\Delta A_{i-1}B_{i-1}A_i$ and $\Delta A_{i-1}B_{i-1}C$ are isosceles triangles, we have

$$A_{i-1}B_{i-1} = 2A_{i-1}A_i \cos(\gamma/2), \text{and}$$
$$A_{i-1}C = 2A_{i-1}B_{i-1} \cos(\gamma/2).$$

Therefore, $A_iC = A_{i-1}C - A_{i-1}A_i = A_{i-1}C - \frac{A_{i-1}C}{4\cos^2(\gamma/2)} \leq \frac{3A_{i-1}C}{4}$. Later, we will use this inequality to compute an upper bound for k.

For every pair of points $u, v \in S$ let $\lambda_{u,v}$ be the smallest distance between a pair of non-overlapping parallel lines passing through u and v with angle of inclination $90° + \frac{\gamma j}{2}$, for some positive integer j, e.g., see Figure 14(e). Define λ to be smallest such distance over all $\{u, v\} \in S$. Since the length of A_iC is at most $\frac{3A_{i-1}C}{4}$, for the kth triangle, we have $A_kC \leq \frac{3^kAC}{4^k}$. In the worst case, the length of A_kC is λ. Hence k is bounded by $O(\log(AC/\lambda))$.

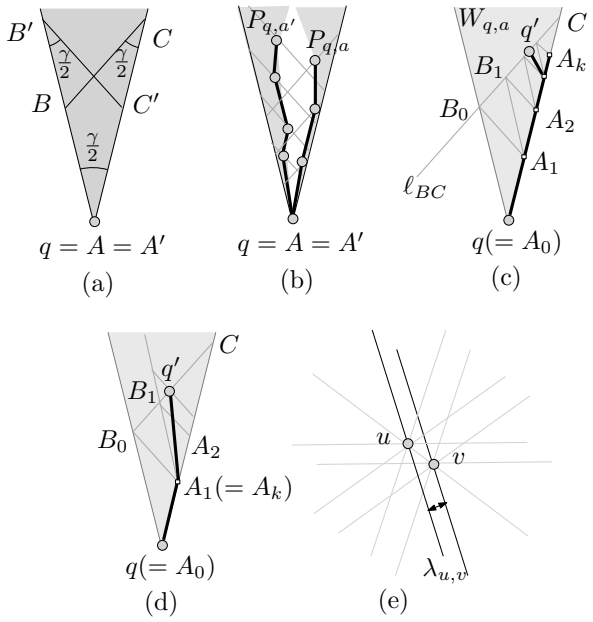

Figure 14: (a) ΔABC and $\Delta A'B'C'$. (b)–(d) Construction of H. (e) $\lambda_{u,v}$.

Lemma 8 *Let q and t be two points in S such that t lies inside $W_{q,a}$. Then there exists an angle-monotone path of width $(\theta_a + \theta_c) = (\theta_{a'} + \theta_{b'}) = \gamma$ between q and t in H.*

Proof: If t lies to the right of $\overline{P}_{q,a}$, then by Lemma 7, there exists an angle-monotone path of width γ between q and t in H.

Consider now the case when t lies to the left of $\overline{P}_{q,a}$. Using an analysis similar to the proof of Lemma 6 we can observe that $P_{q,a}$ and $P_{t,b'}$ must intersect. If they intersect at a vertex v, then the path $t, \ldots, v, \ldots, q$ is an angle-monotone path of width γ. Otherwise, let r be the last vertex on $P_{t,b'}$ to the left of $P_{q,a}$, and let z be the last vertex on $P_{q,a}$ that $W_{z,a}$ contains r. By construction, r is adjacent to a Steiner point s on the right side of $W_{z,a}$. The path $t, \ldots, r, s, \ldots, q$ determines the required angle-monotone path of width γ. □

Let μ be the largest Euclidean distance determined by a pair of points in S, and let $d = (360^\circ/\gamma)$ be an integer. Let $\mathcal{H}$ be the graph obtained by taking the union of Steiner graphs $H_1, \ldots, H_d$, where H_i, $1 \leq i \leq d$, is computed by rotating ΔABC and $\Delta A'B'C'$ clockwise around $A(= A')$ with an angle of $\frac{360^\circ(i-1)}{d}$). Then an analysis similar to the proof of Theorem 2 yields the following result.

Theorem 5 *$\mathcal{H}$ is an angle-monotone graph of width γ, and the number of edges in $\mathcal{H}$ is $O(\frac{n}{\gamma} \log \frac{\mu}{\lambda})$.*

6 Open Questions

1. (from [5]) What is $\gamma_{\min}$, the smallest γ such that every point set has a planar angle-monotone graph of width γ? It is known that $90^\circ < \gamma_{\min} \leq 120^\circ$.

2. We showed that every set of n points admits an angle-monotone graph of width 90° with $o(n^2)$ edges, but can a better bound be proved? Perhaps $O(n \log n)$ edges? Even $O(n)$ is not ruled out.

3. Using Steiner points, we can construct angle-monotone graphs of width γ, for any given $\gamma > 0$, however, the size of the graph depends on some distance parameters of the point set. What is the smallest γ such that every point set has an angle-monotone Steiner graph with width γ and $o(n^2)$ edges?

Acknowledgements

We thank the anonymous reviewers for their detailed feedback to improve the presentation of the paper.

References

[1] S. Alamdari, T. M. Chan, E. Grant, A. Lubiw, and V. Pathak. Self-approaching graphs. In W. Didimo and M. Patrignani, editors, *Proc. of the 20th International Symposium on Graph Drawing (GD)*, volume 7704 of *LNCS*, pages 260–271. Springer, 2013. doi:10.1007/978-3-642-36763-2.

[2] Y. Bahoo, S. Durocher, S. Mehrpour, and D. Mondal. Exploring increasing-chord paths and trees. In J. Gudmundsson and M. H. M. Smid, editors, *Proc. of the 29th Canadian Conference on Computational Geometry (CCCG)*, 2017.

[3] M. W. Bern, D. Eppstein, and J. R. Gilbert. Provably good mesh generation. *Journal of Computer and System Sciences*, 48(3):384–409, 1994. doi:10.1016/S0022-0000(05)80059-5.

[4] C. J. Bishop. Nonobtuse triangulations of PSLGs. *Discrete & Computational Geometry*, 56(1):43–92, 2016. doi:10.1007/s00454-016-9772-8.

[5] N. Bonichon, P. Bose, P. Carmi, I. Kostitsyna, A. Lubiw, and S. Verdonschot. Gabriel triangulations and angle-monotone graphs: Local routing and recognition. In Y. Hu and M. Nöllenburg, editors, *Proc. of the 24th International Symposium on Graph Drawing and Network Visualization (GD)*, volume 9801 of *LNCS*, pages 519–531. Springer, 2016. doi:10.1007/978-3-319-50106-2.

[6] N. Bonichon, C. Gavoille, N. Hanusse, and D. Ilcinkas. Connections between Theta-graphs, Delaunay triangulations, and orthogonal surfaces. In D. M. Thilikos, editor, *Proc. of the 36th International Workshop Graph Theoretic Concepts in Computer Science (WG)*, volume 6410 of *LNCS*, pages 266–278, 2010. doi:10.1007/978-3-642-16926-7_25.

[7] P. Bose, P. Carmi, S. Collette, and M. H. M. Smid. On the stretch factor of convex Delaunay graphs. *Journal of Computational Geometry*, 1(1):41–56, 2010. doi:10.20382/jocg.v1i1a4.

[8] P. Bose, J. D. Carufel, P. Morin, A. van Renssen, and S. Verdonschot. Towards tight bounds on theta-graphs: More is not always better. *Theoretical Computer Science*, 616:70–93, 2016. doi:10.1016/j.tcs.2015.12.017.

[9] P. Bose, R. Fagerberg, A. van Renssen, and S. Verdonschot. Competitive routing in the half-θ_6-graph. In Y. Rabani, editor, *Proc. of the 23rd ACM–SIAM Symposium on Discrete Algorithms (SODA)*, pages 1319–1328, 2012. doi:10.1137/1.9781611973099.

[10] P. Bose, R. Fagerberg, A. van Renssen, and S. Verdonschot. Optimal local routing on Delaunay triangulations defined by empty equilateral triangles. *SIAM Journal on Computing*, 44(6):1626–1649, 2015. doi:10.1137/140988103.

[11] P. Bose, R. Fagerberg, A. van Renssen, and S. Verdonschot. Competitive local routing with constraints. *Journal of Computational Geometry*, 8(1):125–152, 2017. doi:10.20382/jocg.v8i1a7.

[12] P. Bose and P. Morin. Competitive online routing in geometric graphs. *Theoretical Computer Science*, 324(2-3):273–288, 2004. doi:10.1016/j.tcs.2004.05.019.

[13] P. Bose, P. Morin, I. Stojmenović, and J. Urrutia. Routing with guaranteed delivery in ad hoc wireless networks. *Wireless networks*, 7(6):609–616, 2001. doi:10.1023/A:1012319418150.

[14] L. P. Chew. There is a planar graph almost as good as the complete graph. In *Proc. of the 2nd Annual Symposium on Computational Geometry (SoCG)*, pages 169–177, 1986. doi:10.1145/10515.10534.

[15] H. R. Dehkordi, F. Frati, and J. Gudmundsson. Increasing-chord graphs on point sets. *Journal of Graph Algorithms and Applications*, 19(2):761–778, 2015. doi:10.7155/jgaa.00348.

[16] P. Erdös and G. Szekeres. A combinatorial theorem in geometry. *Compositio Math.*, 2:463–470, 1935.

[17] A. Lubiw and D. Mondal. Construction and local routing for angle-monotone graphs. In A. Brandstädt, E. Köhler, and K. Meer, editors, *Proc. of the 44th International Workshop on Graph-Theoretic Concepts in Computer Science (WG)*, volume 11159 of *LNCS*, pages 356–368. Springer, 2018. doi:10.1007/978-3-030-00256-5_29.

[18] A. Lubiw and J. O'Rourke. Angle-monotone paths in non-obtuse triangulations. In J. Gudmundsson and M. H. M. Smid, editors, *Proc. of the 29th Canadian Conference on Computational Geometry (CCCG)*, 2017.

[19] K. Mastakas and A. Symvonis. On the construction of increasing-chord graphs on convex point sets. In N. Bourbakis, G. A. Tsihrintzis, and M. Virvou, editors, *Proc. of the 6th Int. Conf. on Information, Intelligence, Systems and Applications (IISA)*, pages 1–6. IEEE, 2015. doi:10.1109/IISA.2015.7388028.

[20] G. Narasimhan and M. Smid. *Geometric spanner networks*. Cambridge University Press, 2007.

[21] M. Nöllenburg, R. Prutkin, and I. Rutter. On self-approaching and increasing-chord drawings of 3-connected planar graphs. *Journal of Computational Geometry*, 7(1):47–69, 2016. doi:10.20382/jocg.v7i1a3.

[22] G. Rote. Curves with increasing chords. *Math. Proc. of the Cambridge Philosophical Society*, 115:1–12, 1994. doi:10.1017/S0305004100071875.

[23] M. Urabe. On a partition into convex polygons. *Discrete Applied Mathematics*, 64(2):179–191, 1996. doi:10.1016/0166-218X(94)00120-3.